Star Formation in Cosmological Hydrodynamical Simulations

Paramita Barai (pbarai@oats.inaf.it), *Matteo Viel*, *Stefano Borgani*, *Luca Tornatore*, *Pierluigi Monaco*, *Giuseppe Murante*,

[INAF - Astronomical Observatory of Trieste]

Klaus Dolag **[univ. Munich]**, *Edoardo Tescari* **[univ. Melbourne]**

Methodology

- We perform cosmological hydrodynamical simulations
- 3D Tree-PM SPH code Gadget-3 (Springel 2005)

- Cosmological volume, with periodic boundary conditions, evolved using [dark matter + gas] particles
  - From z = 99, up to z = 2
  - Concordance ΛCDM parameters

- Baryonic subgrid physics included :

  - Metal-dependent radiative cooling (Wiersma et al. 2009)

  - Star formation, using effective subresolution model of multiphase ISM (Springel & Hernquist 2003)

$$\rho_{SF} = 0.13 \text{ cm}^{-3}$$

  - Stellar evolution & chemical enrichment (Tornatore et al. 2007)

- Kinetic feedback from SNe-driven galactic outflows using new observationally-constrained sub-resolution models (Barai, Viel, et al. 2012):

  - Radially varying wind where the outflow velocity has a positive correlation with galactocentric distance (Steidel et al. 2010)
  - Additional dependence on halo mass (Martin 2005)

Table 1. Simulations Parameters [a]

Run Name	$L_{\rm box}$ [b] $[h^{-1}$ Mpc]	$N_{\rm part}$ [c]	$m_{\rm gas}$ [d] $[h^{-1}M_\odot]$	$L_{\rm soft}$ [e] $[h^{-1}$ kpc]	Galactic Wind Feedback
		Smaller-Box Runs : SB [f]			
NWt	5	2×128^3	7.66×10^5	0.98	No Wind
CWt	5	2×128^3	7.66×10^5	0.98	Energy-driven constant-velocity $v = 400$ km/s
RVWat	5	2×128^3	7.66×10^5	0.98	Radially varying with fixed parameters [g]
RVWbt	5	2×128^3	7.66×10^5	0.98	RVW with halo mass dependent parameters [h]
		Larger-Box Runs : LB [i]			
NW	25	2×320^3	6.13×10^6	1.95	No Wind
CW	25	2×320^3	6.13×10^6	1.95	Energy-driven constant-velocity $v = 400$ km/s
RVWa	25	2×320^3	6.13×10^6	1.95	Radially varying with fixed parameters [g]
RVWb	25	2×320^3	6.13×10^6	1.95	RVW with halo mass dependent parameters [h]

[a] All simulations have the same physics described in §2, with the wind model varied.

[b] $L_{\rm box}$ = Comoving side of cubic simulation volume.

[c] $N_{\rm part}$ = Number of gas and DM particles in the initial condition.

[d] $m_{\rm gas}$ = Mass of gas particle (which has not undergone any star-formation).

[e] $L_{\rm soft}$ = Gravitational softening length (of all particle types). The minimum gas smoothing length is set to a fraction 0.001 of $L_{\rm soft}$.

[f] Run names ending with "t" are smaller boxsize runs SB, stopped at $z \sim 2$.

[g] Parameters of radially varying wind model (§2.3): $r_{\rm min} = 1h^{-1}$ kpc, $R_{\rm eff} = 100h^{-1}$ kpc, $v_{\rm max} = 800$ km/s, $\alpha = 1.15$.

[h] Parameters of radially varying wind model dependent on halo mass (§2.3): $v_{\rm max} = 2\sqrt{GM_{\rm halo}/R_{200}}$, and $R_{\rm eff} = R_{200}$.

[i] Runs with larger boxsize LB, stopped at $z \sim 2$.

Galaxy Gas & Stellar Mass Function & Mass Fraction at z ~ 2

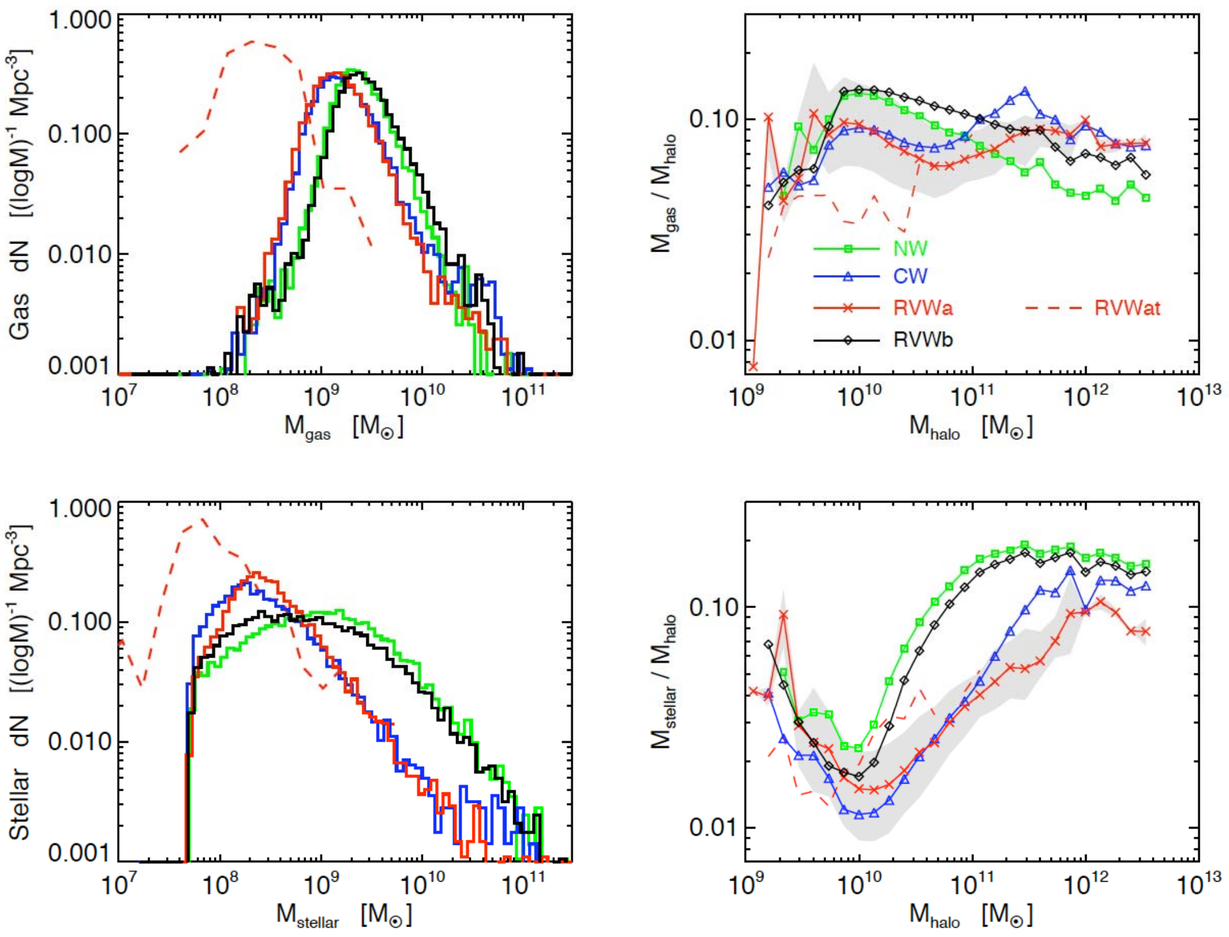

Figure --- Galaxy gas mass function (*top-left panel*), stellar mass function (*bottom-left*), along with gas mass fraction (*top-right*) and stellar mass fraction (*bottom-right*) w.r.t. total mass of halos, at z = 2.23, of the LB runs shown as the solid curves.

In the *right panels* the solid curves denote the median value within a mass bin for each run, and the grey shaded area enclose the 70th percentiles above and below the median in run RVWa (red curve) showing the typical scatter.

One of the wind model (RVWat) from the SB box is plotted as the *red dashed curve* in each panel ⇒ The smaller higher-resolution box SB extends the gas & stellar mass functions to lower-masses.

Global Star Formation Rate Density (SFRD) Evolution

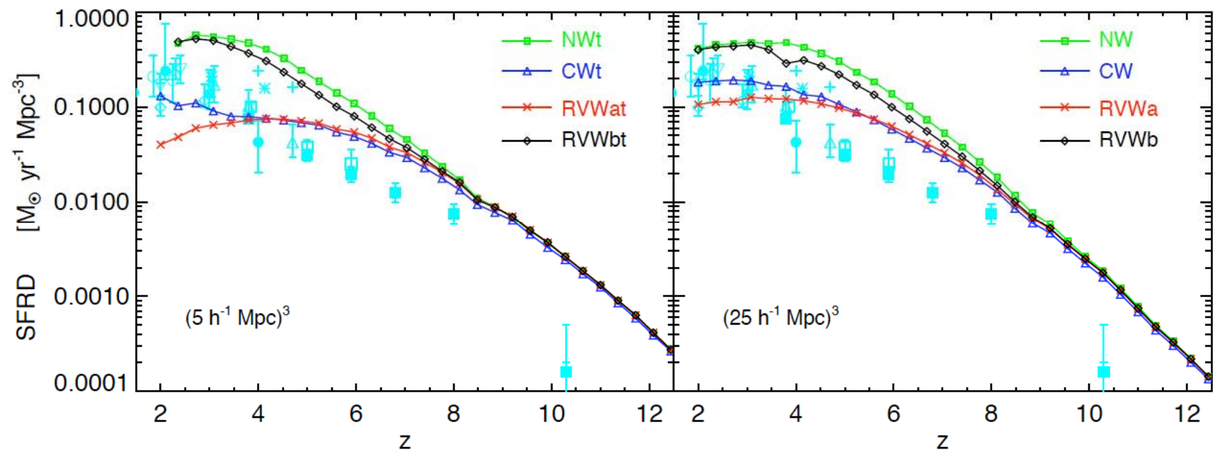

Figure --- SFRD in whole simulation volume as a function of redshift, for the SB runs in the *left* and LB in the *right panel*, with the respective wind models labeled by the colors and plotting symbols. The cyan symbols and error bars denote observational data from:

- Cucciati, O. et al. (2012), A&A, 539, A31 - (*filled circles*),
- Steidel, C. C., et al. (1999), ApJ, 519, 1 - (*asterisks*),
- Ouchi, M. et al. (2004), ApJ, 611, 660 - (*plus signs*),
- Perez-Gonzalez, P. G. et al. (2005), ApJ, 630, 82 - (*inverted triangles*),
- Schiminovich, D. et al. (2005), ApJ, 619, L47 - (*diamonds*),
- Bouwens, R. J. et al. (2009), ApJ, 705, 936 - (*open squares*),
- Reddy, N. A. & Steidel, C. C. (2009), ApJ, 692, 778 - (*crosses*),
- Rodighiero, G. et al. (2010), A&A, 515, A8 - (*open circles*),
- van der Burg, R. F. J. et al. (2010), A&A, 523, A74 - (*upright triangles*),
- Bouwens, R. J. et al. (2012), ApJ, 754, 83 - (*filled squares*).

- Galactic wind feedback has significant impact on SFRD, reducing SFR several times depending on the outflow model

- Box-size and simulation resolution also affects SFRD
  - At z = 12, SFRD is ~ 2 times more in the higher-resolution SB box than LB
  - At z < 3 - 4, the RVWat run of smaller-box SB series produces 2 - 3 times lower SFRD than RVWa of LB

- Shape of SFRD evolution
  - SB box tend to show a peak in SFRD at a certain redshift
  - LB box have a plateau of SFRD between z = 2 - 3.5

- There is a better match of simulations with observations at lower-z
  - At z = 4.5 - 10, SFRD in the simulations is systematically higher, reaching 2 - 10 times the observed values
  - At z = 2 - 4.5, most of the observations lie within the ranges of SFRD produced by the different wind models

References

- Barai, P., Viel, M., et al. 2012, submitted to MNRAS
- Martin, C. L. 2005, ApJ, 621, 227
- Springel, V. & Hernquist, L. 2003, MNRAS, 339, 289
- Springel, V. 2005, MNRAS, 364, 1105
- Steidel, C. C., Erb, D. K., Shapley, A. E., Pettini, M., Reddy, N., Bogosavljevic, M., Rudie, G. C. & Rakic, O. 2010, ApJ, 717, 289
- Tornatore, L., Borgani, S., Dolag, K. & Matteucci, F. 2007, MNRAS, 382, 1050
- Wiersma, R. P. C., Schaye, J. & Smith, B. D. 2009, MNRAS, 393, 99